Journal of Nuclear Materials 392 (2009) 259–263

Contents lists available at ScienceDirect

Journal of Nuclear Materials

journal homepage: www.elsevier.com/locate/jnucmat

An X-ray absorption spectroscopy study of Mo oxidation in Pb at elevated temperatures

Shanshan Liu *, Daniel Olive, Jeff Terry, Carlo U. Segre

Center for Synchrotron Research and Instrumentation, Department of Biological, Chemical and Physical Sciences, Illinois Institute of Technology, 3101 South Dearborn St., Chicago, IL 60616, USA

A B S T R A C T

The corrosion of fuel cladding and structural materials by lead and lead-bismuth eutectic in the liquid state at elevated temperatures is an issue that must be considered when designing advanced nuclear systems and high-power spallation neutron targets. In this work, lead corrosion studies of molybdenum were performed to investigate the interaction layer as a function of temperature by X-ray absorption spectroscopy. *In situ* X-ray absorption measurements on a Mo substrate with a 3–6 μm layer of Pb deposited by thermal evaporation were performed at temperatures up to 900 °C and at a 15° angle to the incident X-rays. The changes in the local atomic structure of the corrosion layer are visible in the difference extended X-ray absorption fine structure and the linear combination fitting of the X-ray absorption near-edge structure to as-deposited molybdenum sample and molybdenum oxide (MoO_2 and MoO_3) standards. The data are consistent with the appearance of MoO_3 in an intermediate temperature range (650–800 °C) and the more stable MoO_2 phase dominating at high and low temperatures.

1. Introduction

Lead and lead-bismuth eutectic (Pb/LBE) have emerged as primary candidates for application in advanced nuclear reactors and transmutation systems as coolants and high-power spallation neutron targets [1–5]. Pb/LBE has a low melting temperature, high boiling temperature and it is chemically inert. However, Pb/LBE is very corrosive to many structural materials, if they are exposed to Pb/LBE directly at medium to high temperatures. This has limited the useful operating range of most Pb/LBE eutectic systems to temperatures around 550–600 °C.

Studies of the corrosion reactions in the Pb/LBE system are important in developing mitigation techniques, corrosion tolerant materials, and coatings. It is known that the formation of a protective oxide layer on the metal surface using controlled amounts of oxygen can protect against dissolution attack by liquid lead-alloys [1]. Liquid metal corrosion of steels has been shown [6–13] to be dependent upon many different parameters including the type of steels, thermal conditioning, the surface treatment of steel, oxygen concentration, application temperature, flow velocity, etc. Fazio et al. [14] and Ilincev et al. [15] reported on the corrosion of steel and refractory metals (W, Mo) by oxygen-controlled flowing LBE. Mo and W, both refractory metals, have the lowest solubility in LBE and exhibit better corrosion resistance than steels. Since corrosion occurs at the surface, corrosion resistance has been increased by alloying Al, Si, or Zr into the steel surface or by maintaining protective films formed by carefully controlling the dissolved oxygen concentration in the molten Pb/LBE [16–22]. However, definite and quantitative methods for preventing corrosion cannot be presented because experimental results are either scarce or when available are under varying conditions.

In this paper, we report the characterization of the local atomic and electronic structures of the corrosion products with molybdenum by X-ray absorption spectroscopy (XAS). XAS is the modulation of the X-ray absorption probability of an atom due to the chemical and physical state of the atom. The XAS is typically divided into two regimes: X-ray absorption near-edge spectroscopy (XANES) and extended X-ray absorption fine-structure spectroscopy (EXAFS). XANES provides qualitative information about formal oxidation state and coordination chemistry of the absorbing atom, while EXAFS allows the determination of the distances, coordination number, and types of near neighbor atoms. XAS has rarely been used to study the properties of Pb corrosion tolerant materials and coatings in the past. However, we show that it is possible to determine the structural changes at the Pb–Mo interface after high temperature treatment. Such an atomistic understanding of the corrosion process can be extended to other systems and will assist in improving the development of corrosion resistant materials and coatings.

* Corresponding author. Tel.: +1 312 567 5955; fax: +1 312 567 3494.
E-mail address: liushan1@iit.edu (S. Liu).

0022-3115/$ - see front matter © 2009 Elsevier B.V. All rights reserved.
doi:10.1016/j.jnucmat.2009.03.005

2. Experimental

2.1. Sample preparation

These *in situ* experiments were carried out in a specially designed tube furnace insert (Fig. 1(a)) with three Kapton windows, permitting the introduction of X-rays along the tube axis and the measurement of fluorescence at 90°. The *in situ* sample was made from a molybdenum rod (99.95% metals basis) machined to present a 15° angle to the incident X-rays (Fig. 1(b)) and coated with a ~3–6 μm layer of Pb (99.999% metals basis) by thermal evaporation. The thickness of the Pb layer was estimated by knowing the total mass of Pb evaporated and using the equation $\delta = m\cdot\cos(\theta)/4\pi\rho r^2$, where δ is the thickness, m is the total Pb mass, ρ is the density of Pb, r is the distance between the evaporation source and the substrate, and θ is the longitude (azimuthal angle). θ was zero since the source was positioned directly below the substrate. Fig. 2 shows the insert inside the furnace in the Materials Research Collaborative Access Team (MR CAT) experimental station. The same sample was heated sequentially to 400, 500, 700, 750, 800, 850, and 900 °C under flowing Ar. The temperature was measured with a thermocouple probe located adjacent to the insert within the tube furnace. An XT16 series temperature controller (ATHENA Controls, ±1% accuracy) was used to control the sample temperature. Samples were held at final temperature for 30 min after which power was disconnected and the furnace was allowed to cool to room temperature for the XAS measurements.

2.2. XAS measurement

Measurements of fluorescence and XAS spectra were performed at the MRCAT, Sector 10-beamline at the Advanced Photon Source, Argonne National Laboratory. A cryo-cooled Si (111) monochromator was used to select the X-ray energies for our measurements. A rhodium-coated mirror was used to reject the higher harmonics from the monochromator. The absorption from the Mo K-edge (20.0004 keV) was measured. The energies of the X-rays were calibrated using a Mo foil as a standard. The XAS measurements were performed in fluorescence geometry with a 19-element Ge detector perpendicular to the incident beam. Under these conditions, we estimate that the incident X-rays are probing approximately 1–3 μm below the Pb/Mo interface. Enhanced surface sensitivity was obtained by making measurements with the excitation beam at a grazing angle (15°) of incidence. At 15°, there remains a significant spectral contribution from bulk molybdenum.

3. Results and discussion

Fig. 3 shows Pb L_α fluorescence spectra taken from an *in situ* Mo/Pb sample at different temperatures. The *in situ* Pb fluorescence measurements on the Mo/Pb sample indicate that the Pb remains on the surface at all temperatures. The integrated intensity of the Pb fluorescence peak shows only a small reduction as a function of processing temperature.

3.1. EXAFS analysis

XAS analysis was performed using the IFEFFIT interactive software package (with ATHENA and ARTEMIS graphical interfaces) [23]. The Mo K-edge data were processed using ATHENA for background subtraction by fitting linear polynomials to the pre-edge and the post-edge region of an absorption spectrum, respectively. The $\chi(E)$ data were converted into k-space (E_0 was taken at 20 keV for the sample), k-weighted, and Fourier transformed between $k = 2$–11 Å^{-1} using a Hanning window, into R-space. Due to reduced amplitude because of the self-absorption in the thick molybdenum metal substrate, self-absorption corrections have been applied to the data using the Booth and Bridges algorithm [24] in ATHENA. The parameters used for this calculation are the incident and outgoing angles in degrees (15° and 75°) and the thickness of the sample in microns (5 μm was used as it is larger than the estimated X-ray penetration).

The $\chi(R)$ functions (related to the radial distribution) obtained from the Mo K-edge XAFS data are presented in Fig. 4. Data from three processing steps (only as-deposited, 700 and 900 °C data are presented for clarity) show that the molybdenum probed by the X-rays remains largely metallic (see the fit from Fig. 5) but with additional intensity below ~2.0 Å due to the formation of short-range order during the high temperature processing. This is an indication that a structural change occurred in the samples during processing to high temperature. Because the X-rays incident at 15° probe a significant depth below the Mo/Pb interface, removal of the large metallic Mo signal is required to extract the short distance information. Therefore, the raw data at all processing temperatures were fit to a Mo metal structural model as follows. First, all scattering paths, including multiple scattering, were generated using ARTEMIS between 1.6 and 5.6 Å. The paths were calculated using crystallographic data available for Mo metal [25] in the body-centered cubic structure. Next, the best fit was obtained by allowing only four parameters to vary: the edge energy shift (E_0), the overall amplitude reduction factor (S_0^2), an isotropic expansion factor (α), and a disorder parameter (β) which was used to scale the mean squared disorder for each path to its length. Fig. 5 displays the fit to the as-deposited Pb-coated molybdenum rod data collected at room temperature using this highly constrained model. The R-factor of the fit shown in Fig. 5 is 0.046.

The Mo EXAFS data obtained after each high temperature processing step were fit using the same method as for the as-deposited sample shown in Fig. 5 with similar R-factors and quality of fit. The fit was subtracted from the experimental data to obtain a

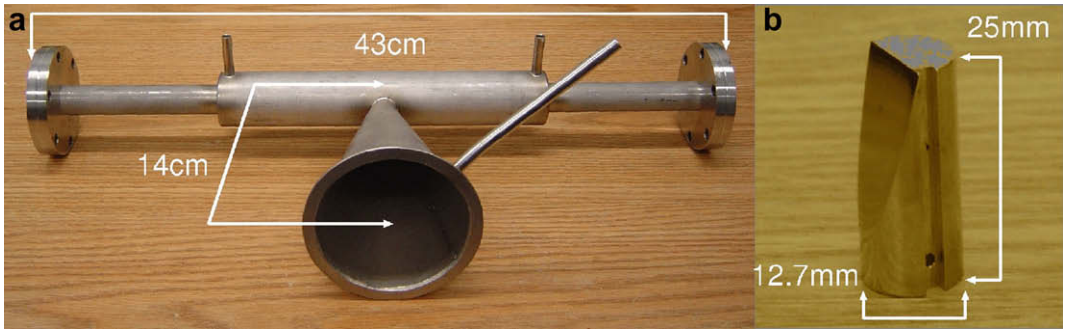

Fig. 1. High temperature furnace insert (a) and molybdenum rod sample with 15° angled side surface (b).

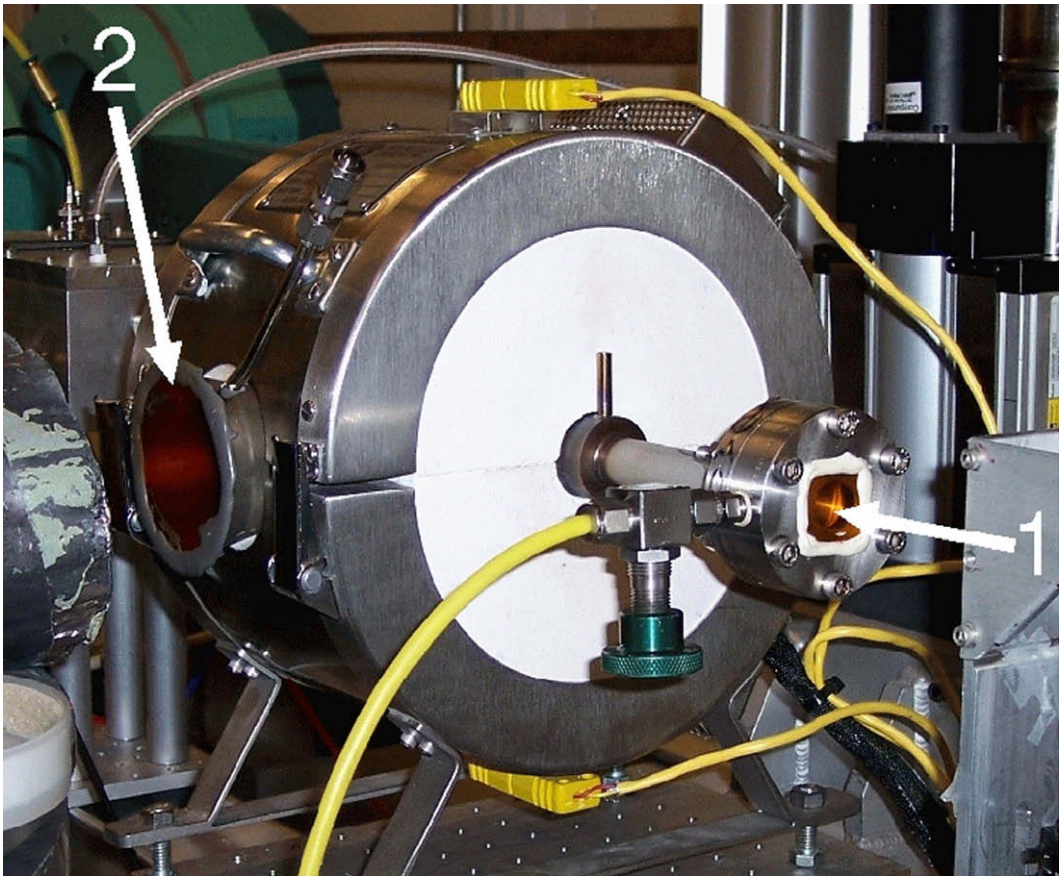

Fig. 2. Furnace, with insert, installed in the MRCAT experimental station. X-rays are incident along arrow 1 and the Kapton-sealed fluorescence window is shown by arrow 2.

difference spectrum, which provides a qualitative measure of the change in the low-*R* intensity as a function of processing temperature. Fig. 6 shows the residual of $\chi(R)$ at k^3 weighting for selected temperatures. The low-*R* peaks exhibit a systematic growth in intensity to a maximum at 750 °C but disappear at higher temperatures. This is suggestive of chemical interactions occurring at the Mo/Pb interface, but the limitation of having a 15° incident X-ray angle prevents a more detailed structural analysis of the EXAFS data.

3.2. XANES analysis

XANES analysis has been performed on the Mo K-edges from the sample. The comparison of the normalized spectra in the XANES range of Mo/Pb sample at different processing temperature shows changes in the shape and intensity of features observed near the edge region.

Fig. 7 depicts the Mo K-edge XANES spectra from the as-deposited Mo/Pb sample, and heat treatments of 400, 500, 700 and

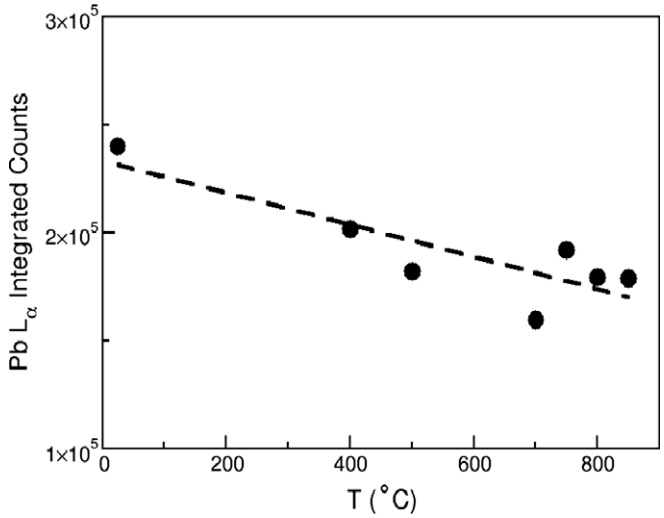

Fig. 3. Integrated intensity of the Pb L_α fluorescence taken on *in situ* samples vs. temperature, error bars fall inside the symbols.

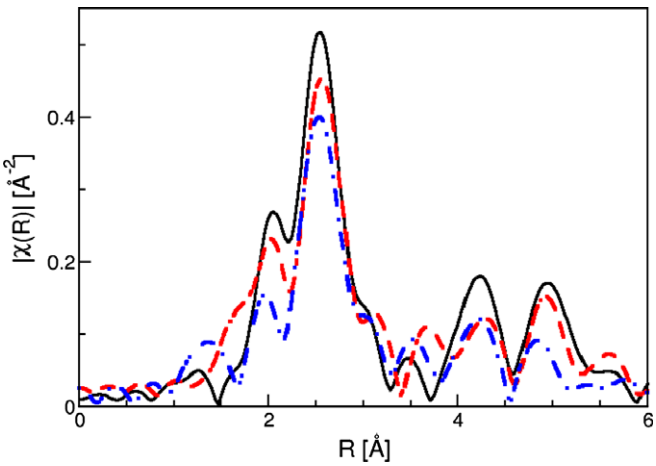

Fig. 4. Mo $\chi(R)$ vs. temperature for selected heat treatments: as-deposited (—); 700 °C (– – –); 900 °C (–·– ·).

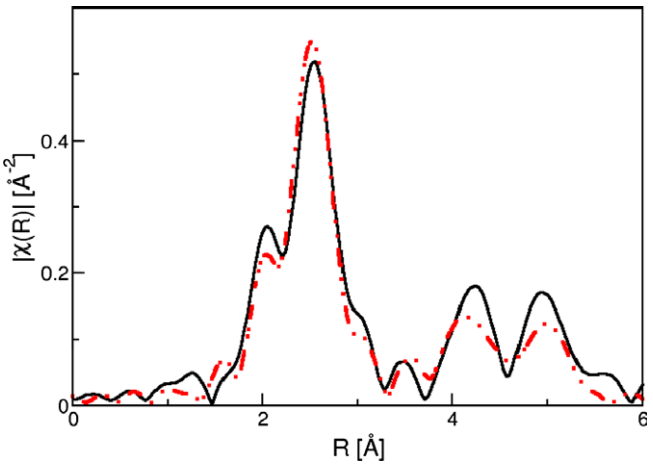

Fig. 5. Comparison of the as-deposited Mo/Pb sample experimental $\chi(R)$ data (—) to the fit (–··) using a constrained pure Mo structural model over the range, 1.6 Å < R < 5.6 Å.

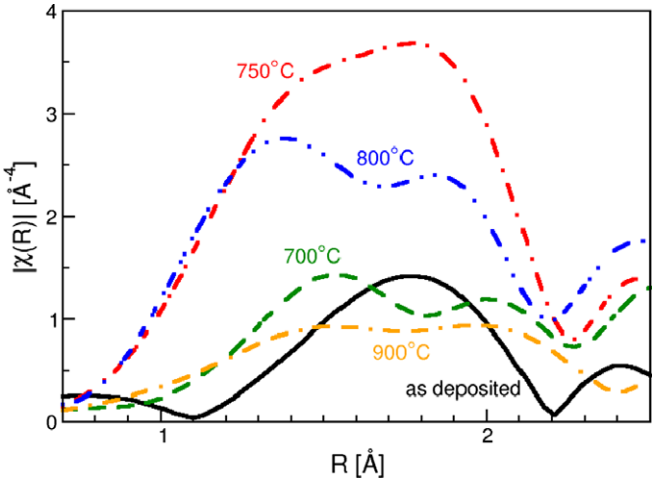

Fig. 6. Residual $\chi(R)$ at k^3 weighting after removing Mo metal fit for Mo/Pb sample treated at different temperatures: as-deposited (—); 700 °C (– – –); 750 °C (–· – ·); 800 °C (–··) and 900 °C (– – ·).

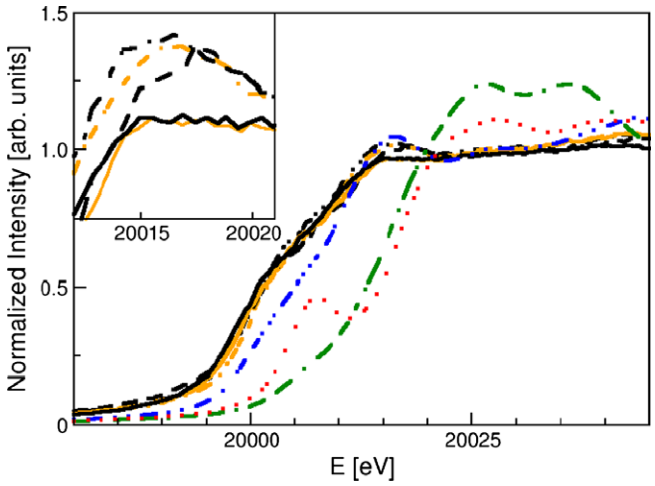

Fig. 7. Mo XANES comparison of Mo/Pb sample, as-deposited (black – · – ·), 400 °C (grey – · – ·), 500 °C (black – – –), 700 °C (grey —), and 900 °C (black —) with standards of Mo foil (··–); MoO_2 (– – ·); and MoO_3 (····). (color) Mo XANES comparison of Mo/Pb sample, as-deposited (black – · – ·), 400 °C (orange – · – ·), 500 °C (black – – –), 700 °C (orange —), and 900 °C (black —) with standards of Mo foil (blue · ·–); MoO_2 (green – – ·); and MoO_3 (red · · · ·) (For interpretation of the references to color in this figure legend, the reader is referred to the web version of this article.).

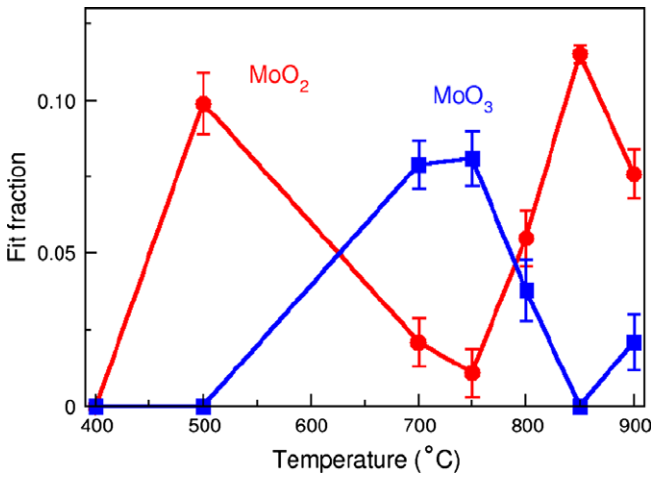

Fig. 8. MoO_2 (circle) and MoO_3 (square) component fit fractions versus temperature obtained from least squares fitting of the XANES data. The dominant component is the spectrum of the as-deposited sample (~0.90, not shown).

900 °C compared with the spectra from three reference samples, Mo foil, MoO_2, and MoO_3. Comparison of the measured spectra to the corresponding references reveals very similar features for the sample with increasing processing temperature except for the decrease of the 'white line' peak at 20,015 eV. In order to quantify this effect, the experimental XANES spectra were analyzed by linear combination least-squares fitting in ATHENA, using the initial Mo/Pb metal sample, MoO_2, and MoO_3 as reference standards to extract information about the oxide composition at the Mo/Pb interface. The least squares fits were dominated by the spectrum of the as-deposited sample (~0.90 fit fraction) however some systematic trends can be seen in the extracted oxide fractions as a function of temperature (Fig. 8). At low temperatures MoO_2 begins to form at the interface. At intermediate temperatures, the MoO_2 is converted to MoO_3 which remains most stable until its melting temperature (800 °C). Finally, MoO_2 reappears and dominates above 800 °C. This demonstrates that, despite relatively deep penetration of the excitation X-ray beam at the 15° incident angle into the bulk molybdenum, this measurement is sensitive to the Mo either at the buried interface or dissolved in the Pb overlayer.

4. Conclusions

The local environment of *in situ* molybdenum that was exposed to lead was investigated by Mo K-edge XAS. This technique has been shown to be sensitive to the surface chemistry of the Mo as a function of temperature. The EXAFS and XANES data show similar trends with the qualitative appearance and disappearance of a short distance peak (EXAFS) and the quantitative signature of the MoO_3 moiety (XANES) in the intermediate temperature range of 650–800 °C. The 15° incident angle limits the quantitative analysis of the EXAFS due to the dominant components arising from bulk Mo, however, our results indicate that lower angle and, more specifically angle-dependent measurements, will permit the development of a detailed picture of the evolution of corrosion at the buried Mo/Pb interface and that this technique can be extended to other relevant structural materials.

Acknowledgments

This research was supported by DOE NERI Grant No. DE-FC07-05ID14674. MRCAT operations are supported by the Department of Energy and the MRCAT member institutions. Use of the Advanced Photon Source at Argonne National Laboratory was supported by the US Department of Energy, Office of Science, Office of Basic Energy Sciences, under Contract No. DE-AC02-06CH11357. We would like to thank Dr A.J. Kropf of Argonne National Laboratory for the use of the tube furnace and insert in this work.

References

[1] B.F. Gromov, Yu.S. Belomitcev, E.I. Yefimov, M.P. Leonchuk, P.N. Martinov, Yu.I. Orlov, D.V. Pankratov, Yu.G. Pashkin, G.I. Toshinsky, V.V. Chekunov, B.A. Shmatko, V.S. Stepanov, Nucl. Eng. Des. 173 (1997) 207.
[2] B.W. Spencer, in: Proceedings of 8th International Conference of Nuclear Engineering, ICONE-8, April 2–6, Baltimore, MD, USA, 2000.
[3] M. Salvatores, G.S. Bauer, G. Heusener, PSI-Report Nr. 00–05, Paul Scherrer Institut, Villigen, Switzerland, 2000.
[4] Jinsuo Zhang, Ning Li, Review of Studies on fundamental issues in LBE corrosion LA-UR-04-0869, 2004.
[5] Eric P. Loewen, Am. Scient. 92 (2004) 522.
[6] F. Barbier, G. Benamati, C. Fazio, A. Rusanov, J. Nucl. Mater. 295 (2001) 149.
[7] F. Barbier, A. Rusanov, J. Nucl. Mater. 296 (2001) 231.
[8] G. Benamati, C. Fazio, H. Piankova, A. Rusanov, J. Nucl. Mater. 301 (2002) 23.
[9] Y. Kurata, M. Futakawa, K. Kikuchi, S. Saito, T. Osugi, J. Nucl. Mater. 301 (2002) 28.
[10] Y. Kurata, M. Futakawa, J. Nucl. Mater. 325 (2004) 217.
[11] Y. Kurata, M. Futakawa, S. Saito, J. Nucl. Mater. 343 (2005) 333.
[12] Jinsuo Zhang, Ning Li, Yitung Chen, A.E. Rusanov, J. Nucl. Mater. 336 (2005) 1.
[13] Masatoshi Kondo, Minoru Takahashi, J. Nucl. Mater. 356 (2006) 203.
[14] C. Fazio, I. Ricapito, G. Scaddozzo, G. Benamati, J. Nucl. Mater. 318 (2003) 325.
[15] G. Ilincev, D. Karnik, M. Paulovic, A. Doubkova, J. Nucl. Mater. 335 (2004) 210.
[16] Allen L. Johnson, Eric P. Loewen, Thao T. Ho, Dan Koury, Brian Hosterman, Umar Younas, Jenny Welch, John W. Farley, J. Nucl. Mater. 350 (2006) 221.
[17] L. Soler Crespo, F.J. Martín Muñoz, D. Gómez Briceño, J. Nucl. Mater. 296 (2001) 273.
[18] G. Müller, A. Heinzel, J. Konys, G. Schumacher, A. Weisenburger, F. Zimmermann, V. Engelko, A. Rusanov, V. Markov, J. Nucl. Mater. 301 (2002) 40.
[19] G. Müller, A. Heinzel, J. Konys, G. Schumacher, A. Weisenburger, F. Zimmermann, V. Engelko, A. Rusanov, V. Markov, J. Nucl. Mater. 335 (2004) 163.
[20] Eric P. Loewen, Hannah J. Yount, Kevin Volk, Arvind Kumar, J. Nucl. Mater. 321 (2003) 269.
[21] Y. Kurata, M. Futakawa, S. Saito, J. Nucl. Mater. 335 (2004) 501.
[22] Annette Heinzel, Masatoshi Kondo, Minoru Takahashi, J. Nucl. Mater. 350 (2006) 264.
[23] B. Ravel, M. Newville, J. Synchrotron Rad. 12 (2005) 537.
[24] C.H. Booth, F. Bridges, Physica Scripta T115 (2005) 202.
[25] R.W.G. Wyckoff, Cryst. Struct. 1 (1963) 7.